JOURNAL OF MORPHOLOGY 221:25–43 (1994)

Comparative Study of Lower Pharyngeal Jaw Structure in Two Phenotypes of *Astatoreochromis alluaudi* (Teleostei: Cichlidae)

A. HUYSSEUNE, J.-Y. SIRE, AND F.J. MEUNIER
National Fund for Scientific Research, Institute of Zoology, University of Ghent, B-9000 Ghent, Belgium (A.H.); URA CNRS 1137, Laboratoire d'Anatomie comparée, Université Paris 7, F-75251 Paris Cedex 05, France (J.-Y.S., F.J.M.); Laboratoire d'Ichtyologie générale et appliquée, Muséum national d'Histoire naturelle, F-75231 Paris Cedex 05, France (F.J.M.)

ABSTRACT The potentially molluscivorous East-African cichlid *Astatoreochromis alluaudi* is known to exhibit phenotypic plasticity in its pharyngeal jaw apparatus. We examined wild-caught (snail-eating) fish and specimens experimentally reared on soft food for differences in bone structure in their lower pharyngeal jaw (LPJ). The LPJ is built up of two halves, each of which consists of four structural units: a bony dentigerous, sutural and cortical plate, surrounding a medullary cavity containing sparse bone. Histomorphometric data and associated statistical analysis on serial microradiographs through the posterior third region of the LPJ, where crushing forces are assumed to be the highest, reveal differing growth trajectories: (1) compensating for fish size (standard length) the LPJ grows to a significantly larger size and volume in snail-eating specimens, (2) all structural units distinguished contribute to the volume increase of the LPJ in the hard versus the soft phenotype, and (3) the bone volume fraction in each of the units keeps pace with the growth of the unit proper, indicating that porosity does not change on one growth trajectory or from one phenotype to another. In addition, morphological observations show in hard food specimens: (1) the development of a structurally different bony layer along the inner side of the cortical plate, and (2) a reinforcement of the medullary cavity in the form of oriented trabeculae. Both are interpreted as a consolidation of the medullary cavity to resist the compressive forces exerted when hard food particles (mollusc shells) are crushed.

Pharyngeal jaws in cichlids and in related pharyngognath families are a second pair of jaws located deep in the buccopharyngeal cavity and developmentally derived from the second to fifth branchial arches (Nelson, '69; Liem and Greenwood, '81; Vandewalle et al., '94). The paired upper pharyngeal jaws and single lower pharyngeal jaw start their development as cartilaginous masses and rods in early ontogeny, but bone and tooth formation are soon initiated and the pharyngeal jaws rapidly become large, predominantly bony, toothed elements (Huysseune, '89). For further information on the developmental origin, form, and function of pharyngeal jaws in general, and of cichlids in particular, see Vandewalle et al. ('94).

The lower pharyngeal jaw (LPJ) and its dentition have long been considered a valuable diagnostic taxonomical feature, especially in cichlids (e.g., Greenwood, '81; Trewavas, '83; Kullander, '84 and refs. therein; Casciotta and Arratia, '93). The LPJ in cichlids presents conspicuous differences in form and dentition that have been related to the trophic specialization of the species concerned (piscivores, intrapharyngeal mollusc-crushers, insectivores, etc.) (Barel et al., '77).

Astatoreochromis alluaudi is a common cichlid species of East-African lakes and rivers of the Lake Victoria drainage system (Greenwood, '59). It feeds predominantly either on snails (by crushing them between its pharyngeal jaws) or on insects. Greenwood ('59) described the two types, which differ in

Address reprint requests to A. Huysseune, Instituut voor Dierkunde, Ledeganckstraat 35, B-9000 Ghent, Belgium.

form of the pharyngeal bones, and interpreted them as subspecies because they were confined to different lakes. Later, Greenwood ('65) reported the shape changes of the pharyngeal jaws when a descendent from a wild specimen of a Lake Victoria population (showing extreme pharyngeal hypertrophy, see below) was raised under laboratory conditions on a soft, snail-free diet. Hoogerhoud ('84, '86) found considerable differences in the morphology of the LPJ (bone shape and dentition) of this species from 40 mm standard length (SL) onward, according to whether the specimens were collected in lakes where they feed on soft food items such as insects or in lakes such as Lake Victoria where they feed on snails. Specimens feeding on insects had a rather small, slender LPJ, whereas specimens feeding on snails had a large and stout (so-called hypertrophied) LPJ (cf. also Greenwood, '59). According to Hoogerhoud's ('86) data, such differences could indeed be contrived experimentally in tanks within one generation. The polymorphism in the LPJ could therefore be phenotypical, and Hoogerhoud ('86) suggested that the differences in LPJ development were most likely caused by pressure on the bone resulting from the crushing activity of the pharyngeal jaw apparatus (and not by the extra calcium delivered by snail shells, a suggestion made by Greenwood, '65). Ever since Greenwood's ('65) study, several reports have demonstrated the variability in cichlid pharyngeal jaw morphology as a result of phenotypic plasticity or as expressions of genetic polymorphisms (e.g., Eccles and Lewis, '79; Loiselle, '79; Lewis, '82; Kornfield and Taylor, '83; Meyer, '89, '90a,b; Witte et al., '90).

Of the upper and lower pharyngeal jaws, mostly the LPJ has been used in studies dealing with pharyngeal jaw variability in cichlids (but see Barel et al., '76) because of its (1) shape and structure reflecting conspicuously the functional importance of the pharyngeal jaws in feeding, (2) supposed taxonomical importance, and (3) easier accessibility.

Until now, only external shape and size measurements have been used to characterize differences between phenotypes (e.g., Hoogerhoud, '84, '86; Kornfield, '91). The aim of the present work is to describe and quantify the differences in bone structure of the lower pharyngeal jaw in *Astatoreochromis alluaudi* in relation to the diet and to generate hypotheses on the possible morphogenetic mechanism responsible for the divergence of phenotypes at a certain stage of development.

MATERIALS AND METHODS

Eleven wild-caught specimens of *Astatoreochromis alluaudi* from the Mwanza Gulf (Lake Victoria), ranging from 53 to 101 mm SL, were taken to represent the hard food phenotype. It is known that the populations in this lake mainly feed on the thick-shelled gastropod *Melanoides tuberculata* (Müller) (Greenwood, '65; Hoogerhoud, '86). Eight specimens, ranging from 65 to 86 mm SL, raised in small and shallow ponds (250–525 m^2 surface, ~1 m deep) in an aquaculture station in Northern Cameroon (Slootweg et al., '93), were used as the soft food phenotype. These specimens belonged to filial generations from laboratory-reared animals, deriving from the Mwanza Gulf population. In these ponds, they fed on benthic and/or pelagic organisms and few or no (soft-shelled) snails (Slootweg, pers. comm.).

Additional data were collected from preliminary investigations on three hard food (wild-caught) specimens (75–98 mm SL) and three soft food (laboratory-reared) specimens (73–101 mm SL). All material was fixed in formaldehyde 4% and stored in alcohol 70% prior to processing for ground sections.

In addition, one laboratory-reared specimen (41 mm SL), a descendent from the Mwanza Gulf population, was used for the preparation of serial semithin sections and fixed accordingly in a mixture of 1.5% glutaraldehyde and 1.5% paraformaldehyde following Sire ('85).

For the preparation of semithin sections, the specimen was decalcified in EDTA (cf. Sire, '85), dehydrated, and embedded in epon. Two μm sections were cut with a glass knife and stained with toluidine blue.

For the preparation of ground sections, the LPJs were dissected free from the head and manually cleaned from adhering soft tissues. To enable localization of the ground sections, dorsal views were drawn using a camera lucida. Subsequently the LPJs were dehydrated and embedded in polyester resin (Cronolita 2195 = Stratyl, Rhone-Poulenc). After final hardening the blocks were serially sectioned with a Leitz 1600-saw microtome into slices of 150 ± 15 μm thick, perpendicularly to the anteroposterior axis of the LPJ. Each passage through the saw removes 300 μm of material; therefore the anterior surfaces of subsequent sections were ~450 μm

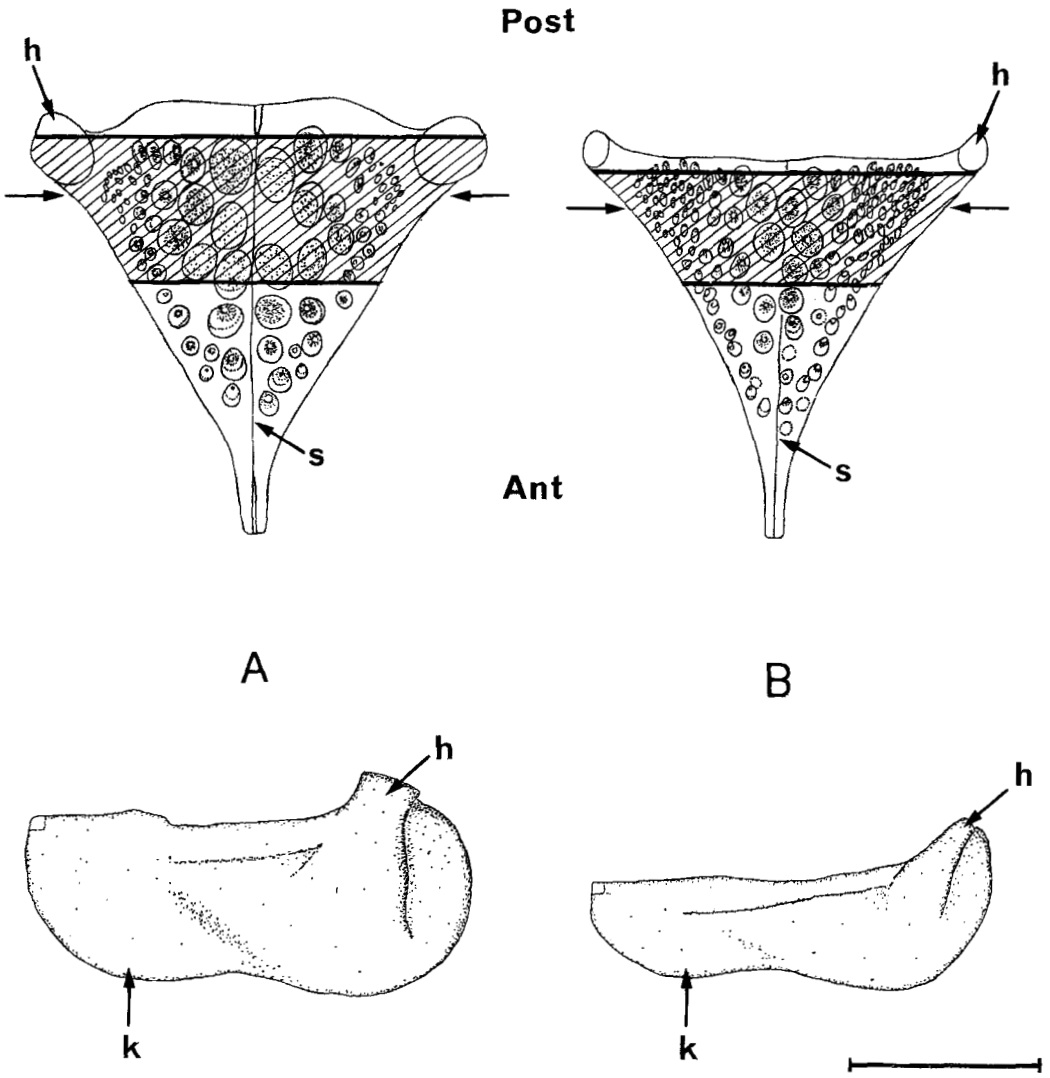

Fig. 1. *Astatoreochromis alluaudi*. Dorsal and lateral views of the LPJ of similar-sized specimens belonging to the two phenotypes (**A** = hard food; **B** = soft food; both 86 mm SL). In the lateral views the teeth are omitted. Hatched area indicates the region selected for study. Arrows indicate the level of the microradiographs presented in Figure 2. Ant, anterior; h, horn; k, keel; Post, posterior; s, suture. Bar = 5 mm.

apart. One specimen of each phenotype was kept for vertical longitudinal (parasagittal) and horizontal longitudinal (frontal) sections after splitting the LPJ into its two symmetrical halves. The ground sections were next microradiographed (10 mA, 30 kV, 30 cm from the source, exposure time 25 min) using a Kodak SO-343 high resolution film. Photographs of the microradiographs were taken on a Reichert Polyvar microscope using an Agfapan APX 25 ASA black and white film.

Of each LPJ, four to nine sections (depending on the anteroposterior LPJ length) were selected in the region covering the three posteriormost (molariform) teeth along the suture (Fig. 1); here the crushing forces are assumed to be the highest. The region covered by these sections represented 30 ± 5% of the anteroposterior length of the LPJ (lower pharyngeal element length, LPL, of Barel et al., '77). All measurements presented here concern that particular selected

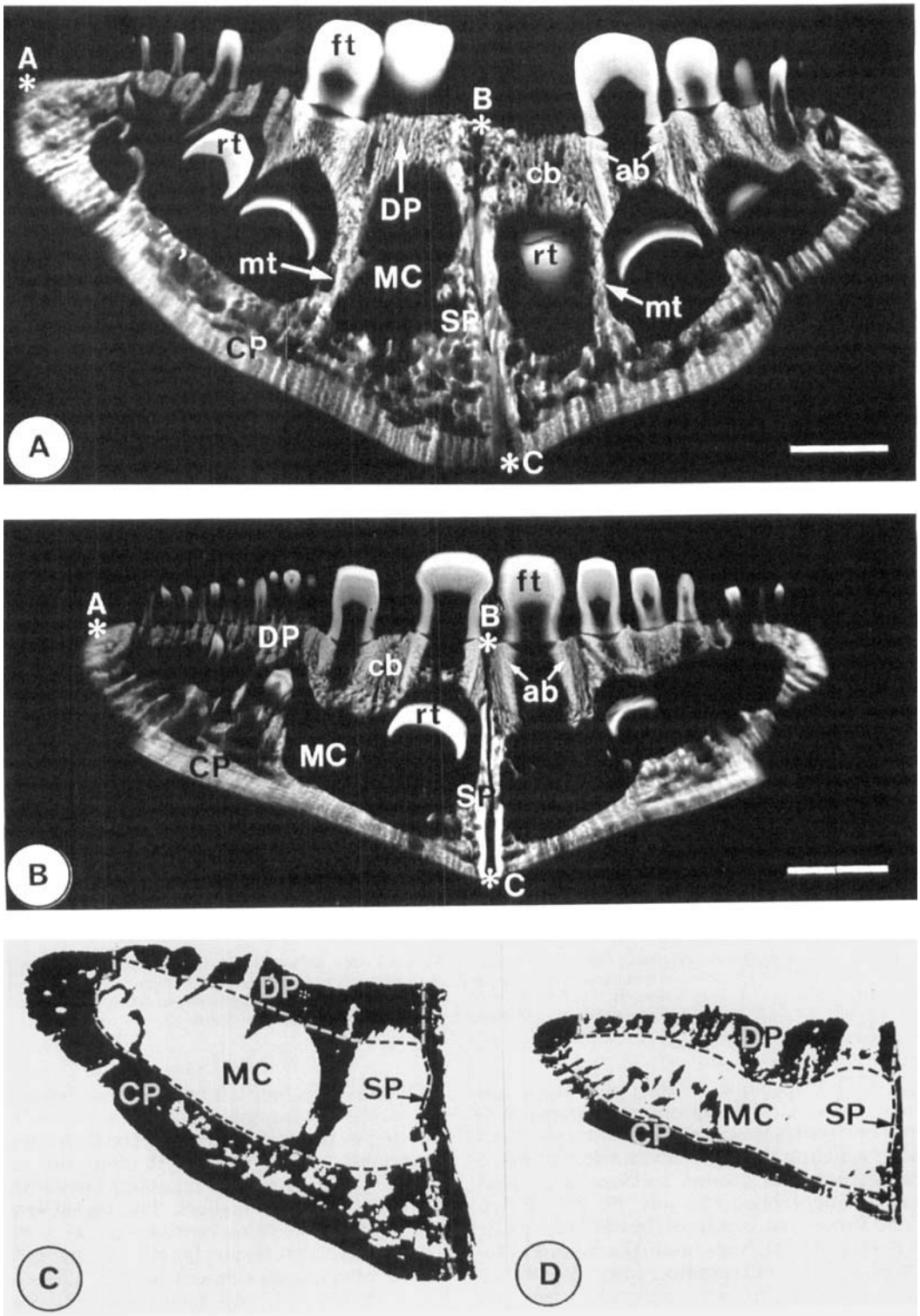
A
ft
B
rt
DP
cb
ab
mt
MC
rt
mt
SP
CP
*C
A
B
ft
A
DP
B
cb
ab
rt
MC
CP
SP
*C
B
DP
MC
SP
CP
C
DP
MC
SP
CP
D

Figure 2

part of the LPJ only. Since preliminary measurements on sections of three hard and three soft food specimens had failed to show any significant differences in area measurements between left and right jaw half, only the left half of a jaw was measured.

Images of the microradiographs of the selected sections were recorded using a CCD video camera Hamamatsu C3077, grabbed by a Neotech Image Grabber NUBus board and stored on the hard disk of a MacIntosh FX computer. Histomorphometric data (lengths, areas of structural units, and areas of bone (vs. voids) within each unit) were collected with the help of a Wacom digitizing tablet, using a software package for image analysis (Optilab 2, Graftek). Four structural units were distinguished according to their localization within the jaw half (the three sides of a triangle plus its center) and because they represent morphological entities: the dentigerous plate dorsally, the sutural plate medially, the cortical plate ventrally, and the medullary cavity centrally (Figs. 2A,B). The following 15 measurements were taken on each section: (1) Three linear measurements: width of the dorsal surface of one LPJ half, length of its cortical plate (CP) and height at the suture (SP) (Fig. 2A,B). For each individual the mean was calculated, yielding the following three variables, respectively: LPJ width, CP length, and SP height. It should be noted that "LPJ width" should not be confounded with "lower pharyngeal element width" (LPW), defined by Barel et al. ('77) as the distance between the caudal tips of the horns. (2) Six area measurements: surface of one-half of the LPJ (LPJ), surface of its three bony units (dentigerous, sutural and cortical plates) taken together (DP + SP + CP) and considered separately (DP, SP, CP), and surface of the medullary cavity (MC). These surface measurements were summed for each individual and transformed to a volume (vol.) by taking 450 μm as the mean section thickness. This yielded the following variables: LPJ vol., DP + SP + CP vol., DP vol., SP vol., CP vol. and MC vol. (3) Six area measurements: surface of the bone in the same six morphological entities as defined in (2). Bone surfaces were measured after a threshold value was determined at a fixed number above mean background darkness (Fig. 2C,D). Surface measurements of the bone (vs. voids) were again summed for each individual but not transformed to a volume, because of the somewhat unpredictable shape of the bone. This yielded the following variables: LPJ bone, DP + SP + CP bone, DP bone, SP bone, CP bone, and MC bone.

Statistical analysis

Linear regressions on standard length were calculated along with their statistics (r^2, F-statistic, and associated probability) for the two diets and the 15 variables described above. To be able to compare regressions of the two diets, 95% confidence limits were calculated on intercept and slope of each individual regression. Furthermore, the point of intersection for each pair of regressions was calculated in the case of nonparallel slopes. Whenever a preliminary analysis of variance showed nonsignificant interaction between diet and standard length, and thus homogeneity of slopes, a more powerful analysis of covariance (ANCOVA, Sokal and Rohlf, '81) was conducted. In these analyses, we evaluated the effect of diet (i.e., category) on the variable considered while taking into account the effect of fish size (standard length thus being the covariate).

Preliminary ANCOVA's were run taking all ($\Sigma N = 117$) separate measurements as independent observations. Although this conservative approach raised the non-explained variance by introducing error, the high number of observations was such that the error mean square became smaller and that the probability level of the F-statistic dropped. Therefore, and because measurements within one individual are not truly independent, measurements, both for regression analysis and ANCOVA, were grouped for each individual, as described above (i.e., as mean, as volume, or as summed bone surface).

All statistics were calculated using the SYSTAT (version 5.0) statistical package

Fig. 2. *Astatoreochromis alluaudi.* Microradiographs of transverse ground sections (viewed from the back) through the LPJ of a hard food (**A**) and a soft food (**B**) specimen at the level indicated in Figure 1. CP, ventral cortical plate; DP, dorsal dentigerous plate with attachment bone (ab) and cancellous bone (cb) and supporting functional teeth (ft); MC, medullary cavity subdivided by bone trabeculae (mt) and containing replacement teeth (rt) in various stages of development; SP, medial sutural plate. A–B = LPJ width (between asterisks); A–C = cortical plate length (between asterisks); B–C = sutural height (between asterisks). Results of image analysis of the left half of the sections presented in A and B are represented in **C** (hard food) and **D** (soft food). Black represents mineralized areas retained after input of a treshold value. Dotted lines in C and D delimit the four structural units (DP, SP, CP, and MC) distinguished in A and B. Bar = 1 mm.

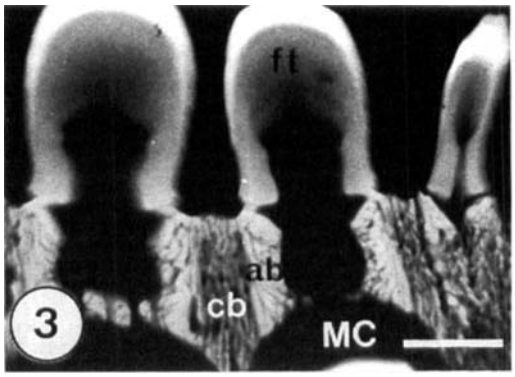

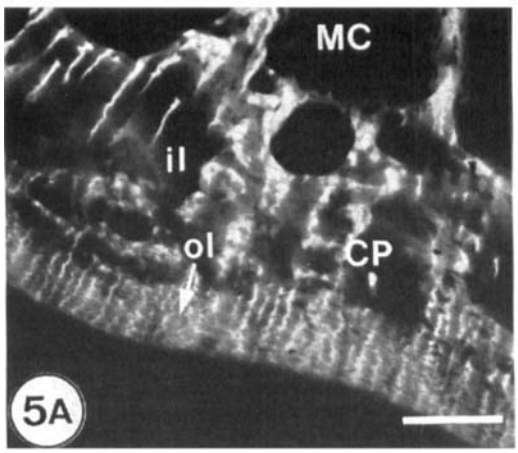

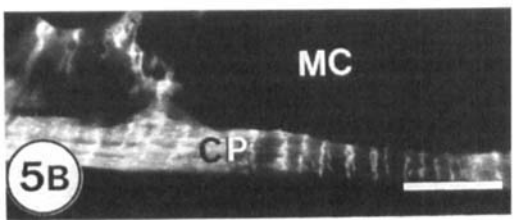

Fig. 3. Microradiograph of transverse ground section through the LPJ of a hard food specimen of *Astatoreochromis alluaudi* (101 mm SL). Detail of the dentigerous plate with cylinders of attachment bone (ab) interconnected by cancellous bone (cb). ft, functional tooth; MC, medullary cavity. Bar = 500 μm.

Fig. 4. Microradiograph of transverse ground section through the LPJ of a hard food specimen of *Astatoreochromis alluaudi* (85 mm SL). Detail of the suture (s) between the two LPJ halves. On one side, the dorsal part of the sutural plate (SP) has been resorbed (arrow). ab, attachment bone within the dentigerous plate; CP, cortical plate; MC, medullary cavity; rt, replacement tooth migrating toward its functional position. Bar = 500 μm.

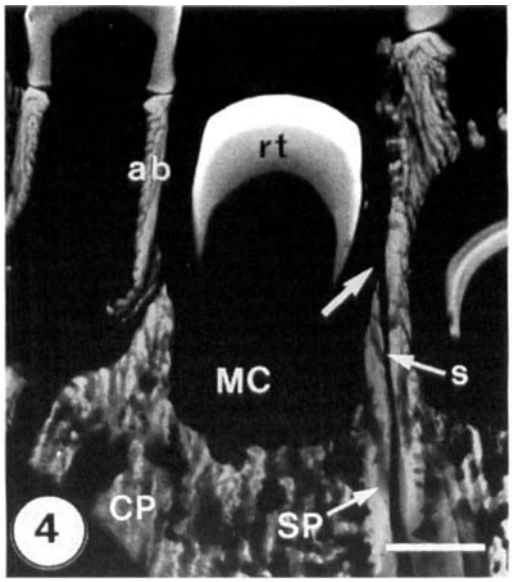

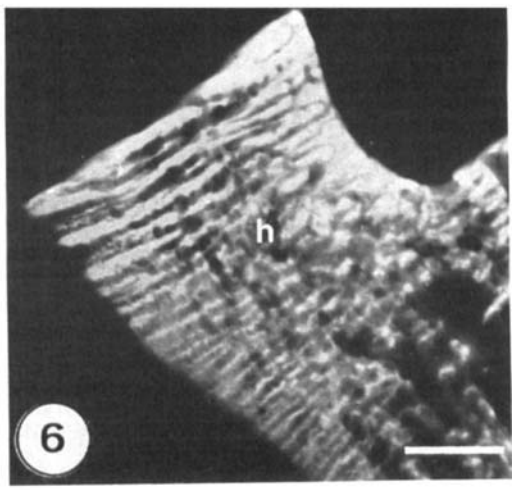

Fig. 5. Microradiographs of transverse ground sections through the LPJ of *Astatoreochromis alluaudi*. Detail showing the bone organization of the cortical plate (CP) in a hard food specimen (**A**, 101 mm SL) compared to a soft food specimen (**B**, 80.5 mm SL). In hard food specimens the cortical plate has a distinct inner (il) and outer (ol) layer. Note the reasonable agreement in size of the outer layer in A and the entire cortical plate in B, taking into account the much smaller standard length of the soft food specimen. MC, medullary cavity. Bar = 500 μm.

Fig. 6. Microradiograph of transverse ground section through the LPJ of a hard food specimen of *Astatoreochromis alluaudi* (101 mm SL). Detail showing the structure of the horn (h). Bar = 500 μm.

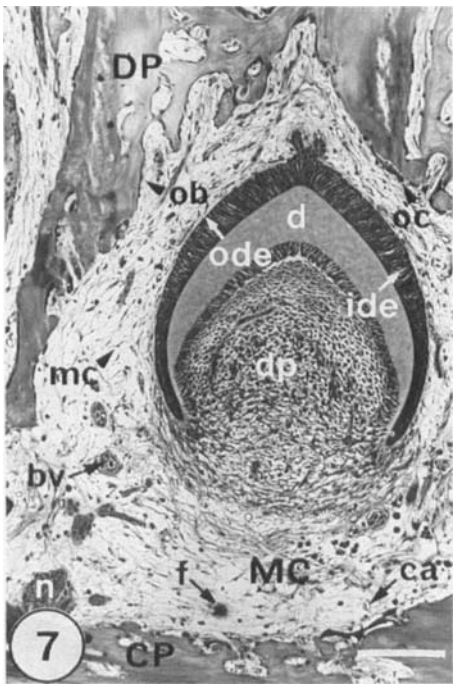

Fig. 7. Micrograph of a transverse semithin (2 μm) section through the LPJ of a soft food specimen of *Astatoreochromis alluaudi* (41 mm SL). Only part of the medullary cavity (MC) is visible. Note mesenchymal cells (mc), capillaries (ca) and larger blood vessels (bv), nerves (n), and a fat cell (f), all surrounding a replacement tooth germ. The latter consists of a core of dentine (d) capping the mesenchymal dental papilla (dp) and surrounded by the inner (ide) and outer (ode) dental epithelium. CP, cortical plate; DP, dentigerous plate; MC, medullary cavity; ob, osteoblasts; oc, osteoclast. Bar = 100 μm.

(Wilkinson, '90), or were derived from these results following Wonacott and Wonacott ('77).

RESULTS

General description

In a dorsal view the LPJ in each of the two phenotypes has a triangular outline, prominent horns for the attachment of muscles, and a large dentigerous area containing numerous teeth of variable shape, ranging from thin and pointed to large and molariform (Fig. 1A,B). At similar standard length, the LPJ of hard food specimens differs from that of soft food specimens by its much greater depth, its greater anteroposterior length, less concave lateral sides and a conspicuous convex posterior border, and by the presence of less pointed and more molariform teeth along with a larger size of the latter. In both phenotypes, the largest teeth are found in the posterior half of the LPJ and are concentrated along the suture (Fig. 1A,B).

On microradiographs of ground transverse sections, taken in the dentigerous region, the LPJ is seen to be composed of two juxtaposed, more or less symmetrical halves, each of which has a roughly triangular outline (Fig. 2A,B). Whatever the phenotype, or the size of the animal, or the localization in the dentigerous region, the same four structural units can always be recognized in each half: i.e., dentigerous, sutural and cortical plates, and medullary cavity.

The dentigerous plate, which supports the functional teeth, is composed of two types of bone tissue, which are easily distinguishable (Fig. 3). Well-mineralized pillars represent sections through cylinders of compact bone which serve for the attachment of the functional teeth (i.e., attachment bone). Less mineralized cancellous bone interconnects these cylinders. Large voids are sometimes present in the dentigerous plate, representing areas of resorption linked to tooth replacement (Fig. 4). Dorsally the dentigerous plate may have a crenelated surface in relation to the level where new cylinders of attachment bone were fixed (Fig. 2A,B). This is especially pronounced in hard food specimens. The ventral lining of the dentigerous plate has a wavy appearance, due to the presence of resorption areas in relation to growing replacement teeth. Resorption acts on both the compact attachment bone and interconnecting cancellous bone. At the posterior end of the LPJ in hard food specimens, the dentigerous plate bears no functional teeth although tooth germs are present in the medullary cavity below.

The sutural plate is composed of compact bone but the outline facing the medullary cavity is fairly irregular. The medial surfaces of the sutural plates of both LPJ halves are closely adjoined, although not fused. The upper part of the sutural plates is often resorbed and subsequently replaced by cancellous bone in relation to tooth renewal adjacent to the suture (Figs. 2B, 4).

The cortical plate in hard food specimens appears to be composed of two superimposed layers of distinct structure (Fig. 5A). An inner layer lining the medullary cavity consists of a loose meshwork of cancellous bone. Its medullary surface is subjected to resorption linked to replacement tooth formation. An outer layer is composed of vertical regularly

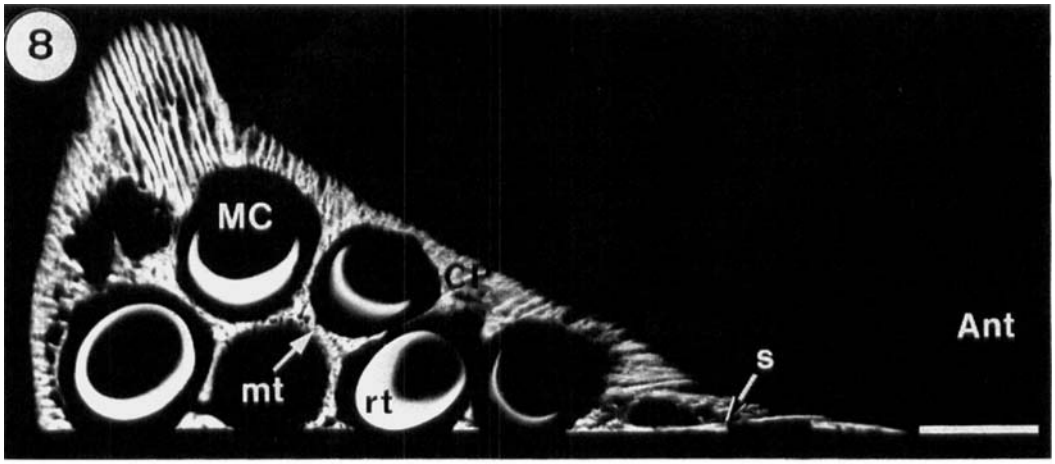

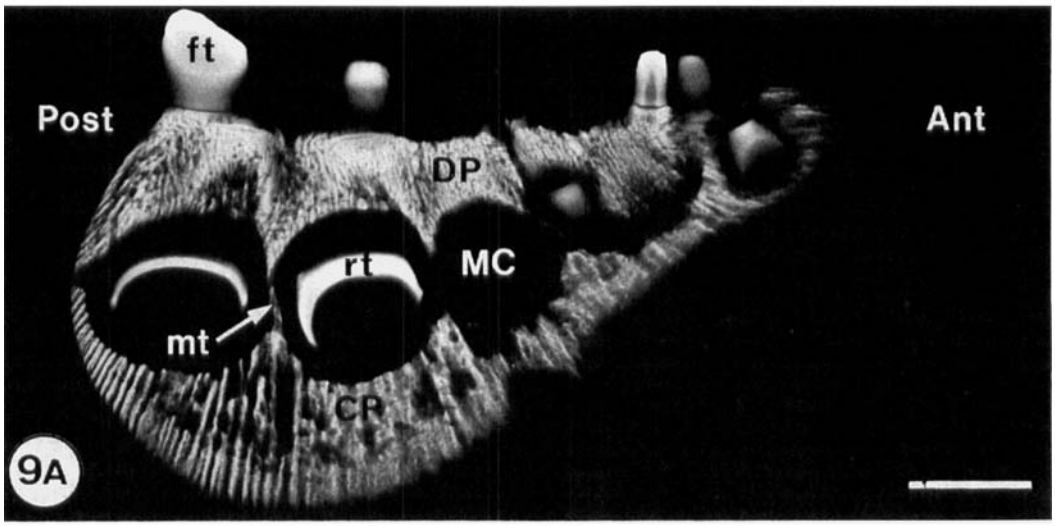

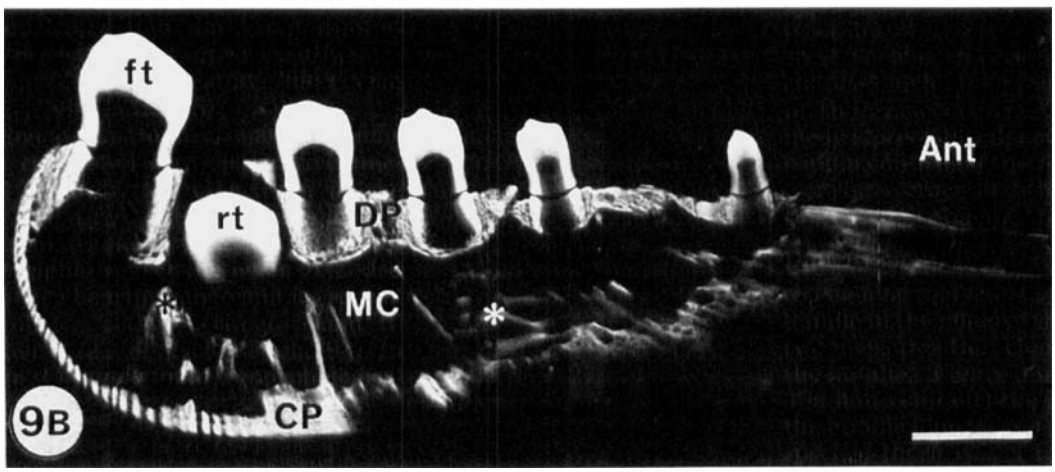

Figures 8–9

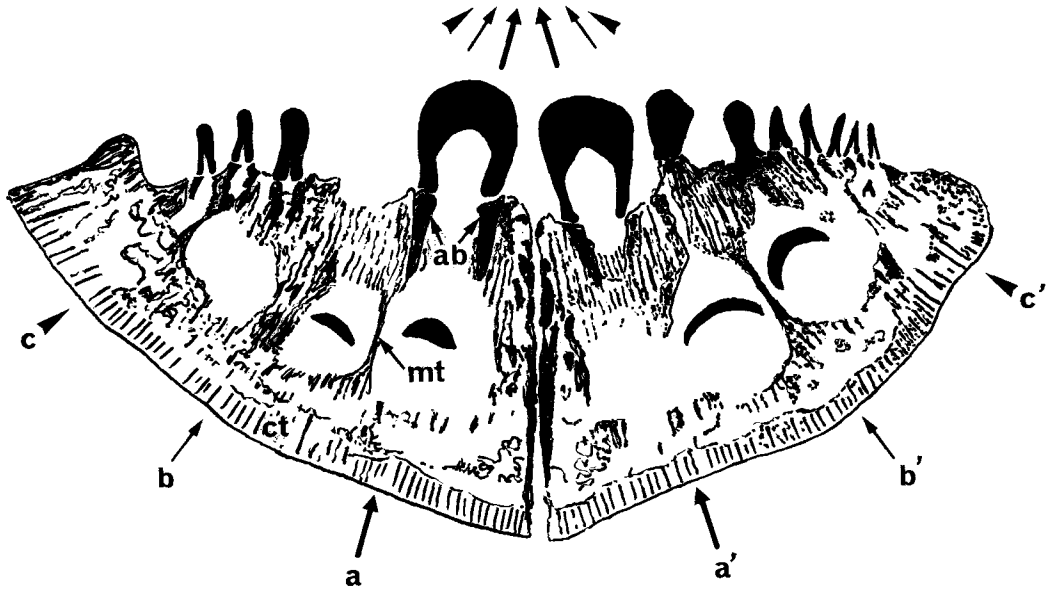

Fig. 10. Schematical drawing of a transverse section of the LPJ of a hard food specimen of *Astatoreochromis alluaudi* showing the preferential orientation of the attachment bone (ab), the medullary trabeculae (mt), and the trabeculae within the cortical plate (ct). Thick arrows indicate the orientation of the attachment bone of the medial tooth and of the cortical trabeculae at the level of a and a'; thin arrows indicate the orientation of medullary and cortical trabeculae at the level of b and b'; arrowheads indicate the orientation of the cortical trabeculae at the level of c and c'. Bar = 1 mm.

spaced thin trabeculae (in average ~50 μm thick), interconnected by thinner perpendicular lamellae. The general picture of the outer layer is that of an oriented cancellous, although slightly porous, meshwork. In soft food specimens the inner layer is weakly, if at all, developed (Fig. 5B). Apart from this difference, the structural organization of the cortical plate is similar throughout the examined dentigerous regions. The ventral side of the cortical plate is fairly smooth throughout the length of the LPJ. The horn lies in the prolongation of the outer layer and shows the same organization, although its surface is highly compact (Fig. 6).

The medullary cavity is filled with a loose meshwork of cellular elements, mostly stellate mesenchymal cells, and contains small capillaries, larger blood vessels, nerves, and fat cells (Fig. 7). Osteoblasts and osteoclasts surround sparse bone. Despite the non-haematopoietic nature of the tissue, the term "medullary" was found suitable as a general term to indicate a central cavity within a bony element (cf. Leeson and Leeson, '76). Especially in hard food specimens, the bone within the medullary cavity takes the form of large bony trabeculae (~250–500 μm thick), which are found throughout the length of the LPJ (Fig. 2A). They connect the cortical plate to the dentigerous plate, where they originate at the basis of two adjacent cylinders of attachment bone (Fig. 2A). The trabeculae

Fig. 8. Horizontal longitudinal (frontal) section through one-half of the LPJ in a hard food specimen (75 mm SL) of *Astatoreochromis alluaudi*. The section is at the level of the medullary cavity (MC). Continuous bony trabeculae (mt) delimit 6 roughly cylindrical crypts in which replacement teeth (rt) develop. Note the trabecular orientation within the cortical plate (CP). Ant, anterior; s, suture. Bar = 1 mm.

Fig. 9. Vertical longitudinal (parasagittal) sections through the LPJ of a hard food (**A**) and a soft food (**B**) specimen of *Astatoreochromis alluaudi* (75 and 76.5 mm SL, respectively). The sections are close to the suture. In B the medullary cavity (MC) does not show trabeculae but an ill-defined cancellous meshwork (*) close to the cortical plate (CP). Note the trabecular orientation within the cortical plate in both specimens. Ant, anterior; DP, dentigerous plate; ft, functional tooth; mt, medullary trabecula; Post, posterior; rt, replacement tooth. Bar = 1 mm.

TABLE 1. Results of linear regression analyses on standard length for all 15 variables and for hard and soft food specimens of Astatoreochromis alluaudi *(upper and lower part of table, respectively)*[1]

Variable	A	cl(A)	B	cl(B)	r^2	F	p
LPJ width	−0.66	1.39	0.06	0.02	0.89	61.45	0.000
CP length	−0.69	1.84	0.07	0.02	0.86	50.99	0.000
SP height	−0.94	1.04	0.05	0.01	0.91	76.42	0.000
LPJ vol.	−51.66	16.14	1.03	0.21	0.94	128.72	0.000
DP + SP + CP vol.	−36.13	11.66	0.70	0.15	0.94	114.69	0.000
MC vol.	−15.53	7.28	0.33	0.09	0.89	63.93	0.000
DP vol.	−8.85	3.32	0.18	0.04	0.92	94.77	0.000
SP vol.	−5.05	2.82	0.10	0.04	0.82	35.74	0.000
CP vol.	−22.23	7.32	0.42	0.09	0.93	106.82	0.000
LPJ bone	−71.64	30.67	1.37	0.40	0.89	63.41	0.000
DP + SP + CP bone	−64.32	28.44	1.23	0.37	0.88	59.29	0.000
MC bone	−7.32	3.72	0.14	0.05	0.85	46.14	0.000
DP bone	−12.40	8.14	0.26	0.11	0.81	32.77	0.000
SP bone	−9.72	5.90	0.18	0.08	0.79	29.14	0.001
CP bone	−42.20	18.87	0.79	0.24	0.87	55.49	0.000
LPJ width	−0.31	1.54	0.05	0.02	0.87	33.33	0.002
CP length	−0.14	1.39	0.05	0.02	0.91	50.70	0.001
SP height	0.62	1.39	0.02	0.02	0.60	7.54	0.040
LPJ vol.	−15.65	7.78	0.38	0.10	0.95	87.34	0.000
DP + SP + CP vol.	−10.68	4.65	0.24	0.06	0.95	95.25	0.000
MC vol.	−4.97	5.31	0.14	0.07	0.84	26.55	0.004
DP vol.	−3.40	2.49	0.09	0.03	0.90	43.29	0.001
SP vol.	−0.40	0.76	0.02	0.01	0.77	16.42	0.010
CP vol.	−6.87	1.98	0.14	0.03	0.97	170.97	0.000
LPJ bone	−21.09	14.68	0.45	0.20	0.87	33.85	0.002
DP + SP + CP bone	−19.48	12.61	0.40	0.17	0.88	37.73	0.002
MC bone	−1.61	2.67	0.04	0.04	0.64	8.95	0.030
DP bone	−6.00	6.50	0.14	0.09	0.77	16.61	0.010
SP bone	−0.65	2.07	0.03	0.03	0.53	5.73	0.060
CP bone	−12.82	4.97	0.24	0.07	0.95	85.66	0.000

[1]Indicated are intercept (A), slope (B), confidence limits (cl) on intercept and slope, coefficient of determination (r^2), F-statistic and associated probability. The variables are: width of the dorsal surface of one LPJ half (LPJ width); length of its cortical plate (CP length); height at the suture (SP height); volume (vol.) and summed bone surface (bone) of respectively one LPJ half in the selected region (LPJ), and of its structural units, taken together (DP + SP + CP), and considered separately (MC, DP, SP, CP). MC, medullary cavity; DP, dentigerous plate; SP, sutural plate; CP, cortical plate.

widen at their points of attachment to the cortical plate. The replacement teeth form between adjacent trabeculae amidst the cellular elements mentioned above (Figs. 2A, 7, 8). The presence of these tooth germs most likely induces resorption of parts of the trabeculae, hence their often irregular shape.

Horizontal longitudinal (i.e., frontal) sections of hard food specimens (Fig. 8) indicate that the trabeculae seen to subdivide the

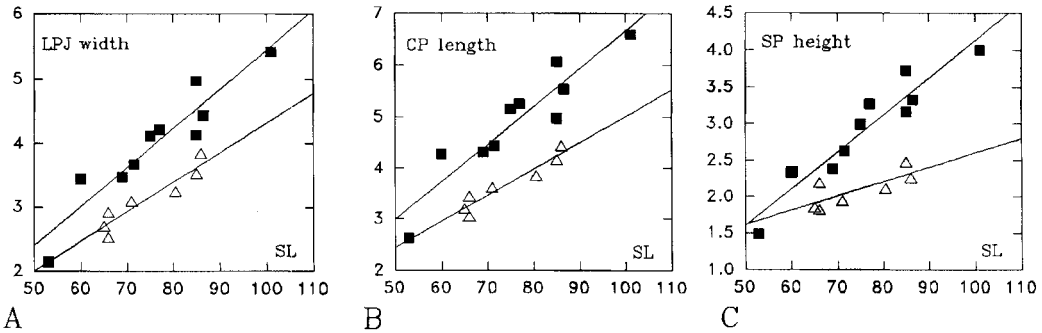

Fig. 11. *Astatoreochromis alluaudi.* Graphs representing the mean, per individual, of (**A**) width of the dorsal surface of one LPJ half (LPJ width); (**B**) length of its cortical plate (CP length); and (C) height at the suture (SP height), in mm, plotted against standard length (SL, in mm) in hard (■) and in soft (△) food specimens (linear regression lines added).

TABLE 2. ANCOVA-results of the following three dependent variables: width of the dorsal surface of one LPJ half (LPJ width); length of its cortical plate (CP length); height at the suture (SP height) in Astatoreochromis alluaudi[1]

Dependent variables	Source of variation	Sum of squares	DF	Mean square	F ratio	P
	Diet	2.35	1	2.35	29.77	0.000
LPJ width	SL	7.56	1	7.56	95.69	0.000
	Error	1.11	14	0.08		
	Diet	4.94	1	4.94	37.98	0.000
CP length	SL	10.68	1	10.68	82.05	0.000
	Error	1.82	14	0.13		
	Diet	2.27	1	2.27	31.89	0.000
SP height	SL	4.34	1	4.34	60.98	0.000
	Error	1.00	14	0.07		

[1]Category: diet; covariate: SL, standard length.

medullary cavity in transverse sections (Fig. 2A) are continuous with one another and with the cortical and sutural plates. They delimit more or less cylindrical crypts in which the replacement teeth develop. Vertical longitudinal (i.e., parasagittal) sections of similar-size specimens show a greater depth of the LPJ and a thicker cortical plate (at least in its posterior third part) in hard (Fig. 9A) than in soft food (Fig. 9B) specimens.

In transverse sections, the trabeculae within three of the structural units described above (dentigerous and cortical plates and medullary cavity) show a similar orientation (Figs. 2A,B, 10). The attachment bone in the dentigerous plate, the trabeculae in the outer layer of the cortical plate, and the large trabeculae in the medullary cavity are all oriented radially with the axes intersecting in a region located above the suture between left and right half of the LPJ (Fig. 10). In frontal (Fig. 8) and in sagittal sections (Fig. 9A,B), cortical trabeculae are oriented predominantly toward a region located approximately in front of the caudal tooth row.

Comparison between the two phenotypes

The linear regressions, calculated for each of the 15 variables, and for hard and soft food specimens, are all statistically highly significant (Table 1), the only exception being the summed bone surface of the sutural plate of soft food specimens, for which the regression nevertheless is nearly significant.

When comparing the two phenotypes, it is clear that hard food specimens have a wider LPJ surface and greater cortical plate length as well as a higher suture for comparable fish sizes (Fig. 11). Because in all three cases neither the slope nor the intercept is significantly different between the two regressions (Table 1), ANCOVA's were run. The results show that, compensating for fish size, the observed variation in each of the three measurements is highly significantly influenced by diet (Table 2).

TABLE 3. Volumes (vol., in mm³) of one-half of the LPJ (i.e., of the region selected in this study) and of its four structural units in hard (n = 10) and soft food (n = 7) specimens of Astatoreochromis alluaudi[1]

SL (mm)	N	LPJ vol. total (mm³)	DP + SP + CP vol. (mm³)	MC vol. (mm³)	DP vol. (mm³)	SP vol. (mm³)	CP vol. (mm³)
53.0	4	3.92	2.59	1.33	1.05	0.35	1.19
60.0	6	12.18	7.91	4.27	2.75	0.96	4.19
69.0	6	15.17	8.93	6.24	2.82	1.04	5.08
71.5	7	19.49	12.42	7.07	3.72	1.56	7.14
75.0	8	28.57	18.14	10.43	5.04	2.70	10.40
77.0	7	27.72	16.51	11.21	4.99	2.19	9.34
85.0	8	27.68	18.87	8.80	5.00	2.12	11.76
85.0	8	38.09	26.01	12.07	6.72	2.48	16.82
86.5	9	38.52	23.47	15.04	7.43	2.63	13.41
101.0	9	54.41	37.30	17.10	10.14	5.65	21.51
65.0	6	9.26	5.23	4.02	2.44	0.65	2.14
66.0	6	8.33	4.59	3.74	2.11	0.67	1.81
66.0	6	10.62	5.20	5.42	2.33	0.74	2.12
71.0	6	10.64	5.54	5.10	2.30	0.64	2.61
80.5	7	13.94	7.66	6.28	3.23	0.78	3.65
85.0	7	17.19	9.51	7.67	3.73	1.08	4.71
86.0	7	17.04	10.15	6.89	4.29	0.98	4.88

[1]N, number of sections corresponding to selected region of LPJ; SL, standard length in mm. Abbreviations as in Table 1.

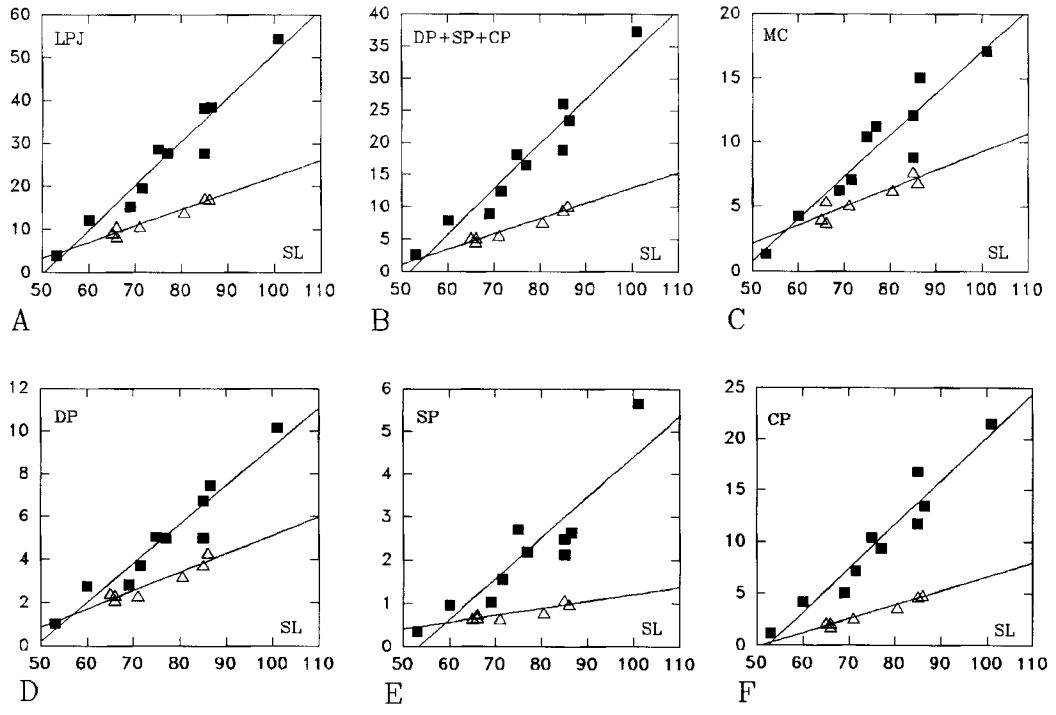

Fig. 12. *Astatoreochromis alluaudi.* Graphs representing the volume of the different structural units (in mm^3) plotted against standard length (SL, in mm) in hard (■) and in soft (△) food specimens (linear regression lines added). **A,** LPJ, one LPJ half in the selected region; **B,** bony units taken together (DP, dentigerous plate; SP, sutural plate; CP, cortical plate); **C,** MC, medullary cavity; **D–F** bony units separately, as abbreviated in B.

Table 3 presents the volumes of one-half of the LPJ (that is, of the region selected for this study), of its three bony units (either taken together or considered separately) and of the medullary cavity, for specimens of both phenotypes. All associated regressions show a significant difference in slope between the two diets (Table 1). It is therefore clear that the selected region of one LPJ half (Fig. 12A) as well as all of its four structural units (Fig. 12C–F) increase in volume to a much larger extent in hard than in soft food specimens. This difference is also obvious when the absolute values of the volumes of the four structural units are presented as stacked-bar diagrams (Fig. 13A). When the volumes are expressed as relative contributions to the LPJ volume the differences between hard and soft food specimens are less pronounced, although the cortical plate appears to be relatively more important in hard food specimens, at the expense of the medullary cavity (Fig. 13B).

Image analysis of the microradiographs after input of the threshold value shows the bone that is retained for area measurements (Fig. 2C,D). Table 4 summarizes these measurements for the different structural units. In addition, the bone areas are calculated as a percentage of the surface of the corresponding unit (= bone volume fraction, i.e., the complement of porosity, cf. Martin, '91). From the graphs of Figure 14, it is clear that the results are very similar to those obtained for the entire structural unit (cf. Fig. 12). All regressions are significantly different in slope between soft and hard food specimens, except for the dentigerous plate. The ANCOVA run for this particular case nevertheless also shows a highly significant effect of diet. This means that both in the entire LPJ (that is, the region selected for this study) (Fig. 14A) and in each of its individual units (Figs. 13C, 14C–F) the summed bone areas increase to a much larger extent in hard than in soft food specimens. However, when represented as bone volume fractions there are no eye-striking differences between hard and soft food specimens (Fig. 15).

The point of intersection for each pair of regression lines (Figs. 12, 14) lies at ~ 55 mm SL (Table 5).

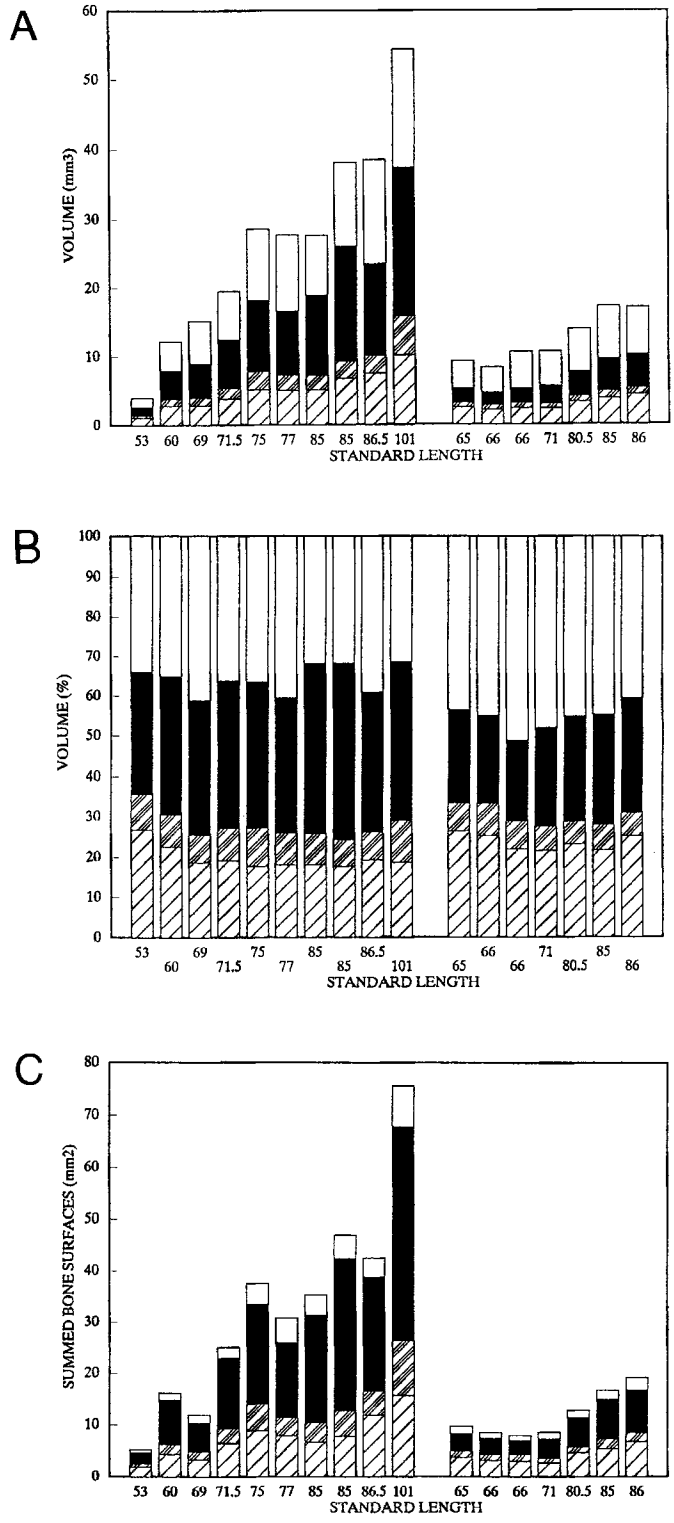

Fig. 13. *Astatoreochromis alluaudi*. **A,B:** Stacked-bar diagrams of absolute (A) and relative (B) values of the volume of the four structural units in the selected region of one LPJ half. **C:** Stacked-bar diagram of the summed bone area per unit. Left 10 bars, hard food specimens; right 7 bars, soft food specimens. /, dentigerous plate; ///, sutural plate; black, cortical plate; white, medullary cavity. Standard lengths are expressed in mm.

TABLE 4. Astatoreochromis alluaudi. *Summed bone surfaces (in mm²) in one-half of the LPJ (i.e., of the region selected) and of the same units as in Table 3. The right four columns represent bone volume fractions for each of the four structural units.*

SL (mm)	N	LPJ bone total (mm²)	DP + SP + CP bone (mm²)	MC bone (mm²)	DP bone (mm²)	SP bone (mm²)	CP bone (mm²)	DP bone (%)	SP bone (%)	CP bone (%)	MC bone (%)
53.0	4	5.25	4.75	0.50	1.95	0.57	2.23	83.69	74.03	84.15	16.89
60.0	6	16.11	14.81	1.30	4.36	1.80	8.65	71.36	84.11	92.81	13.70
69.0	6	11.91	10.32	1.59	3.34	1.48	5.50	53.35	64.35	48.72	11.47
71.5	7	25.04	22.86	2.18	6.45	2.75	13.66	78.09	79.48	86.07	13.87
75.0	8	37.58	33.47	4.11	8.90	5.07	19.50	79.54	84.36	84.38	17.74
77.0	7	30.80	25.90	4.90	7.95	3.39	14.56	71.75	69.75	70.17	19.68
85.0	8	35.30	31.35	3.95	6.70	3.68	20.97	60.36	78.13	80.25	20.19
85.0	8	47.04	42.48	4.56	7.80	4.86	29.82	52.24	88.20	79.80	17.00
86.5	9	42.57	38.75	3.82	11.90	4.55	22.30	72.12	77.78	74.81	11.43
101.0	9	75.54	67.78	7.76	15.69	10.63	41.46	69.64	84.63	86.74	20.42
65.0	6	9.74	8.30	1.44	3.80	1.12	3.38	69.98	77.78	71.01	16.11
66.0	6	8.51	7.45	1.06	3.20	1.13	3.12	68.38	75.84	77.42	12.74
66.0	6	7.97	7.04	0.93	3.08	1.20	2.76	59.46	72.73	58.47	7.72
71.0	6	8.57	7.23	1.34	2.74	0.87	3.62	53.73	61.27	62.52	11.82
80.5	7	12.77	11.39	1.38	4.62	1.11	5.66	64.35	63.79	69.88	9.89
85.0	7	16.68	14.93	1.75	5.44	1.80	7.69	65.70	75.31	73.45	10.26
86.0	7	19.17	16.78	2.39	6.80	1.65	8.33	71.35	75.69	76.85	15.61

DISCUSSION

This report gives one of the first descriptions of the bone structure, at the histological level, of the lower pharyngeal jaw in a teleost fish. Earlier, Meunier and Trébaol ('87) described the structure of the lower pharyngeal jaws in the tropical carangid fish *Trachinotus teraia*. However, these are highly

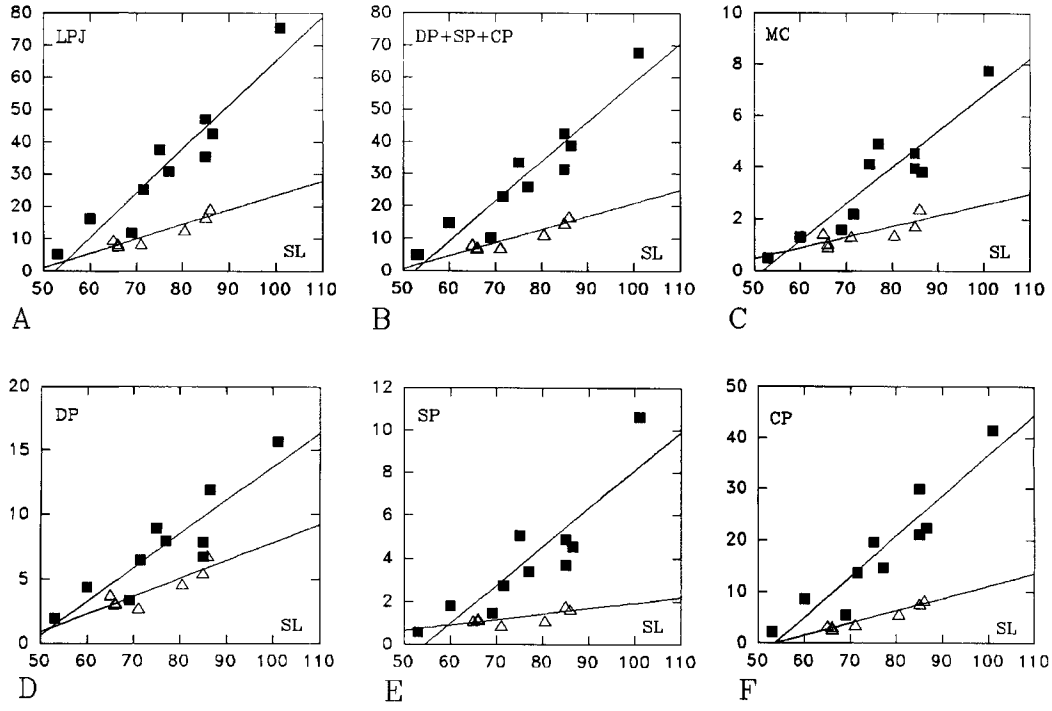

Fig. 14. *Astatoreochromis alluaudi.* Graphs representing summed bone areas in the different structural units (in mm²) plotted against standard length (SL, in mm) in hard (■) and in soft food (△) specimens (linear regression lines added). Abbreviations as in Figure 12.

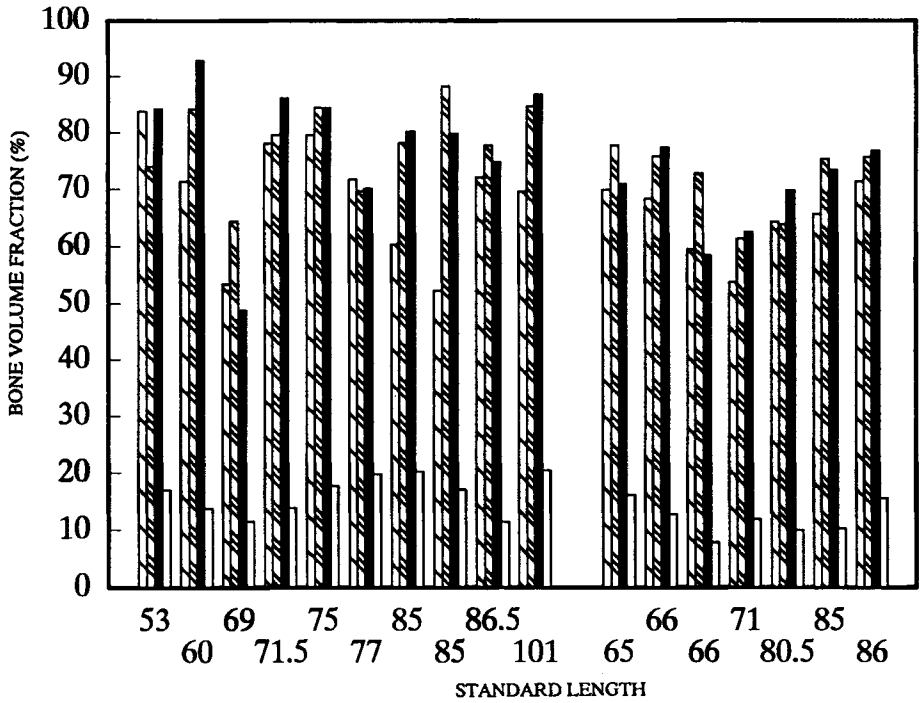

Fig. 15. *Astatoreochromis alluaudi.* Histogram of bone volume fractions (summed bone area per unit as a % of the summed surface of that unit). \, dentigerous plate; \\\, sutural plate; black, cortical plate; white, medullary cavity. Standard lengths are expressed in mm.

modified elements with an edentulous surface, which are made up throughout of vascularized bone tissue in which teeth lie embedded. Our study has been carried out from a comparative perspective with the aim to characterize the effect of different diets on the bone structure at the intraspecific level. It is therefore the first study that examines pharyngeal jaw variability on a structural basis rather than on mere size and shape characteristics (e.g., Hoogerhoud, '86; Kornfield, '91).

TABLE 5. Point of intersection (SL, standard length in mm) of the regressions for hard and soft food specimens of Astatoreochromis alluaudi *and for the twelve variables for which the regressions were significantly different*[1]

Variable	SL
LPJ vol.	55.66
DP + SP + CP vol.	54.96
MC vol.	57.39
DP vol.	56.77
SP vol.	58.75
CP vol.	53.13
LPJ bone	54.77
DP + SP + CP bone	54.49
MC bone	57.70
DP bone	52.02
SP bone	59.68
CP bone	53.60

[1]Abbreviations as in Table 1.

Shape of the LPJ

The shape differences of the LPJ in the two phenotypes, reported earlier by Greenwood ('59) and Hoogerhoud ('84, '86) and confirmed in this study, resemble those found in other snail-eating cichlids known to be polymorphic in their pharyngeal jaws. In the Mexican cichlid *Cichlasoma minckleyi,* the LPJ in papilliform morphs is more delicate, with a significantly narrower outline and smaller horns than the molariform morph (Kornfield and Taylor, '83). These morphs are characterized by a certain degree of trophic specialization, although not very pronounced. *Cichlasoma citrinellum* shows similar differences between papilliform and molariform morphs (Meyer, '90a). As in *A. alluaudi,* the molariform (snail-eating) morph has a clearly deeper LPJ seen from the back than the papilliform morph. Since some of these polymorphisms are believed to be genetically determined (*C. minckleyi,* Kornfield and Taylor, '83; Kornfield, '91) and

others to be at least partially (*C. citrinellum,* Meyer, '90b) or entirely (*Astatoreochromis alluaudi,* Hoogerhoud, '86) phenotypic, there seems to be a striking correspondence between genetically determined pharyngeal jaw polymorphism and phenotypic plasticity in the pharyngeal jaws (Smits et al., pers. comm.).

Bone structure of the LPJ

Because the terminology of bone structure at all levels of organization has obviously been conceived for describing mammalian bone, we have only tentatively used these terms to describe the bone structure of the LPJ in *A. alluaudi,* indicating the differences when appropriate. The architecture of each LPJ half, i.e., a triangle with two sides composed of more or less cancellous bone interconnected by pillars and a third side consisting of a more or less compact plate, is unknown in mammals, and its mechanical implications are as yet unclear.

The dentigerous plate has a compound structure: the cylinders of attachment bone through which the crushing forces are transmitted are compact, whereas the interjacent bone is cancellous, although with some preferential orientation of the bone tissue proper. This compound structure may be a compromise to meet at least two conflicting functional demands: the need to resist crushing forces and the need to have a tissue which is easily remodeled in view of the continuous tooth renewal. According to Currey ('84), cancellous bone of the more oriented type is usually found just underneath loaded surfaces, particularly where the pattern of stress is reasonably constant. Such oriented cancellous bone, although of low porosity, is also found in the outer layer of the cortical plate. Although its trabeculae are oriented radially, the collagen fibrils in these trabeculae as well as the interconnecting lamellae are oriented parallel to the ventral LPJ outline, in the direction of the principal tensile stresses (Huysseune and Sire, unpub. obs.). Indeed, given the fact that the major crushing muscles insert on the horns (Hoogerhoud, '86) and assuming that the prey is crushed close to the suture, in the region of the LPJ where the teeth are stoutest, it is likely that the cortical plate will be subjected to bending. The mechanical significance of an inner, rather unorganized looking, cancellous layer in the cortical plate, especially in hard food specimens, is obscure but may have to do with energy absorption, considering the fact that the medullary trabeculae are anchored within this layer.

Clearly, the tooth directions (except for the most lateral teeth) on the LPJ of *A. alluaudi* of both phenotypes, and the directions of the trabeculae in dentigerous plate, medullary cavity, and cortical plate, all converge toward the medial plane close to the posteriormost functional tooth row. Considering the fact that trabecular organization is almost certainly related to the directions of principal stresses (Currey, '84), the trabecular orientations in the LPJ of *Astatoreochromis alluaudi* may well reflect the direction of major compressive forces, transmitted from a region that is thus considered to be the preferential position for the prey to be crushed. For the zooplanktivore *Haplochromis piceatus,* Galis ('92) found a good agreement between tooth directions on the LPJ along an anteroposterior axis and best biting direction as calculated from a model (i.e., the direction for which the total muscular forces necessary to generate the biting force is minimal).

Effect of diet on jaw architecture

Even when taking into account the differences in fish size in the two samples used, diet has a profound effect upon the size of the LPJ, whether linear measurements are taken or volumes of structural units are considered. The studied region of the jaw grows to a considerably larger size and volume in hard than in soft food specimens. Earlier findings by Hoogerhoud ('86) suggest that the growth trajectories are not distinct from the outset. Hoogerhoud ('86) indeed found a switch in keel depth and horn width, which occurred at the time of a switch in prey type, i.e., ~40 mm SL. The regressions for the two pharyngeal jaw forms obtained in the present study and the intermediate position of the small (53 mm SL), be it single, hard food specimen, support the idea that an ontogenetic switch is responsible for the separation of initially identical fish, which would occur at ~55 mm SL. The differences between Hoogerhoud's observations and ours as to the fish size at which a possible switch occurs may be explained by: (1) the different sample size (that of Hoogerhoud being larger); (2) the different way in which the switch point is determined, with Hoogerhoud's finding being based on Lake Victoria specimens only (small tank-reared and larger wild-caught specimens), the moment of switch of LPJ shape possibly depends on the moment of switch to suitable

hard prey; the switch point we have determined depends on the point of intersection of the two regressions, and therefore on the life conditions in the hard as well as in the soft food specimens; and (3) rates of bone growth and/or remodeling may be differential in different regions of the LPJ. Indeed, keel and horn both serve as insertion areas for the major crushing muscles and are therefore subjected to direct muscular activity, whereas the region of the LPJ that we have measured has primarily a function in resisting compressive crushing forces.

The regression slopes of the unit volumes (Fig. 12) and their relative contributions to the LPJ volume (Fig. 13B) show that all of the four structural units contribute to the volume increase of the LPJ in hard versus soft food specimens, rather than one unit becoming predominant. How do these findings fit in with the profound external shape differences that exist between the two phenotypes? First, these differences are largely determined by an outgrowth of the keel, the development of prominent horns, and the formation of a convex posterior border in hard food specimens, all of which changes have not (or only partially) been quantified here. However, even in the posterior third of the LPJ (i.e., the region studied here), the LPJ is obviously deeper in hard food specimens (cf. Figs. 1, 2A,B). This is reflected in the fact that the difference in regression slopes for the two diets is nearly significant as to sutural height, but not as to LPJ width or cortical length. This is easily explained by the triangular shape of each LPJ half on cross section: increasing sutural height (i.e., deepening of the LPJ) can be realized without affecting the length of the two other sides to the same extent. Deepening of the LPJ is clearly reflected in the considerable volume increase of the sutural plate (Fig. 12E) compared to that of the dentigerous plate and medullary cavity (Fig. 12C,D). The considerable deepening of the LPJ is probably largely realized by a more important development of the cortical plate in hard food specimens (Figs. 12F, 13B), partly at the expense of the medullary cavity. We should mention, however, that cortical plate volume in soft food specimens may possibly be underestimated. Indeed, an ill-defined meshwork, which may have been the forerunner of the inner cortical layer found in hard food specimens, was not incorporated into the unit "cortical plate" but considered sparse medullary bone.

It is perhaps surprising to find that the amount of bone in each of the structural units keeps pace with the volume increase of that unit, i.e., that there are no substantial changes in porosity of the bone, whence the rather similar bone volume fractions in soft and hard food specimens. The discrepancy between the lack of clearly demonstrable differences in medullary cavity bone volume fraction between the two phenotypes, on the one hand, and the obvious presence of distinct medullary trabeculae in hard but not in soft food specimens, on the other hand, may be due, again, to the way in which the medullary and cortical units were delimited. Indeed, the ill-defined meshwork of cancellous bone in soft food specimens (cf. above) was in fact included in the medullary component. Yet, the presence of medullary trabeculae can be interpreted in terms of consolidation of the medullary cavity, preventing it from collapsing when compressive forces are exerted due to crushing hard food particles. Moreover, the widened attachment of the medullary trabeculae to the dentigerous and cortical plates, as well as their localization below the cylinders of attachment bone, permit the stresses to be transmitted to a large area of the cortical plate.

Growth and phenotypic interchangeability of the LPJ

The present study has been conducted to compare functionally similar regions of the LPJ. However, these regions are not necessarily exactly superimposable in hard and soft food specimens: the larger size of this region in hard food specimens may result from mere expansion (internal resorption and external deposition), but most likely also from extra bone having been added posteriorly (cf. the excurved posterior outline of the LPJ in hard food specimens).

Provided that hypertrophy of the LPJ largely results from accelerated growth (cf. Witte et al., '90), as our data suggest, and disregarding the constructional constraints that accommodating a larger LPJ imposes on the entire head (cf. Barel et al., '89), one is inclined to think that it would be easy for a soft food specimen to "switch" to a hard food phenotype according to changing demands. This is further supported by our histological findings (A.H., unpub. obs.): adjustment of LPJ phenotype could easily result from accelerated resorption and/or addition of new bone along the inside of the cortical plate, and accelerated deposition along its outside along

with formation of trabeculae in the medullary cavity. For histological reasons (A.H., unpub. obs.), the reverse phenomenon (resorption taking place at the outside of the cortical plate) seems to be more difficult so that we expect it to be unlikely for a hypertrophied LPJ to become, in absolute terms, a smaller and more slender jaw. The outer size and shape are expected not to change much anymore, although the bony components may become thinner. Therefore, we predict that the growth trajectory of hard food specimens can, at the most, become horizontal (cf. Witte et al., '90) and that, unless the switch "back" is early and unless soft food specimens grow to a very large size, the hard food phenotype cannot converge upon the soft food phenotype, except perhaps for the dentition. Preliminary investigations on two wild-caught specimens (75 and 102 mm SL) fed a soft diet for 6 months seem to confirm this hypothesis. It is interesting at this point to note that Meyer ('87) in his lab-reared *Cichlasoma managuense* found convergence of obtusorostral to acutorostral head shape, but not the reverse. In the case of *C. managuense,* obtusorostral head shape was correlated with flake food and acutorostral with *Artemia* as prey item (Meyer, '87).

Morphogenetic mechanism behind

The changes in LPJ size, shape, and structure once the animal gets on the hard food trajectory are accompanied by changes in the dentition (Hoogerhoud, '84, '86; Huysseune, unpub. obs.). As tooth formation takes place within the medullary cavity of the jaw, the obvious question is whether dentition and bone change synchronously or one precedes the other. In the latter case, are the two causally linked (e.g., do the dentigerous and cortical plates grow apart as a result of pressure exerted by larger tooth germs?) or are both the change in bone and tooth form the mere result of a common signal? Clearly, we must await detailed information on the replacement process and the shape and size of replacement teeth in subsequent tooth generations before these questions can be answered. Hoogerhoud ('86) has earlier suggested that it is the crushing activity of the pharyngeal jaw apparatus and the resulting pressure on the bone, which may be responsible for differences in LPJ development. Since the higher loads imposed on the functional teeth when the fish crushes hard snails are most likely transmitted to the medullary cavity via the cylinders of attachment bone, a hypothesis on how such a signal may act may be that the stresses are captured by the mesenchyme of the medullary cavity. This mesenchyme provides the source for osteoblastic cells that can deposit the medullary trabeculae as well as the cancellous bone of the cortical plate. This mesenchyme most likely also provides the dental papilla cells that participate in replacement tooth formation. Moreover, the medullary cavity also houses capillaries that can deliver the precursors for the osteoclasts. Osteoblasts and osteoclasts govern the process of bone remodeling (Lanyon and Rubin, '85; Marks and Popoff, '88; Vaes, '88; Carter et al., '91) and dental papilla cells are known to instruct the dental epithelium to fold into a particular tooth shape (Kollar, '81).

ACKNOWLEDGMENTS

This study results from a collaboration among the State University of Leiden (The Netherlands), Université Paris 7 (France), and the University of Ghent (Belgium). The *Astatoreochromis* material used for this study was kindly provided by Dr. R. Slootweg, Drs. J. Smits, and Dr. F. Witte, and their colleagues of the University of Leiden. This work greatly benefited from discussions with Dr. K. Desender (Royal Belgian Institute of Natural Sciences, Brussels) on methods of statistical analysis of the data. The authors also thank Prof. Dr. W. Verraes (University of Ghent), Prof. Dr. A. de Ricqlès (Université Paris 7), Dr. C.D.N. Barel, Dr. F. Witte, Drs. J. Smits (University of Leiden), and Dr. K. Desender (R.B.I.N.Sc., Brussels) for their critical comments on earlier drafts, which no doubt greatly improved the manuscript. Mrs. F. Allizard is gratefully acknowledged for assistance in sectioning, and Mrs. R.-M. Servaes for preparation of the photographs. The first two authors acknowledge grants accorded within the frame of an International Program of Cooperation between Belgium (Ministerie van de Vlaamse Gemeenschap; A.H.) and France (CNRS/MRI). A.H. acknowledges a grant of the Fund for Joint Basic Research (FKFO 32.9005.90).

LITERATURE CITED

Barel, C.D.N., F. Witte, and M.J.P. van Oijen (1976) The shape of the skeletal elements in the head of a generalized *Haplochromis* species: *H. elegans* Trewavas 1933 (Pisces, Cichlidae). Neth. J. Zool. *26:*163–265.

Barel, C.D.N., M.J.P. van Oijen, F. Witte, and E. Witte-Maas (1977) An introduction to the taxonomy and morphology of the haplochromine Cichlidae from Lake Victoria. Neth. J. Zool. *27:*333–389.

Barel, C.D.N., G.Ch. Anker, F. Witte, R.J.C. Hoogerhoud, and T. Goldschmidt (1989) Constructional constraint and its ecomorphological implications. Acta Morphol. Neerl.-Scand. *27:*83–109.

Carter, D.R., M. Wong, and T.E. Orr (1991) Musculoskeletal ontogeny, phylogeny, and functional adaptation. J. Biomech. *24:*3–16.

Casciotta, J.R., and G. Arratia (1993) Jaws and teeth of American cichlids (Pisces: Labroidei). J. Morphol. *217:* 1–36.

Currey, J. (1984) The Mechanical Adaptations of Bones. Princeton, N.J.: Princeton University Press.

Eccles, D.H., and D.S.C. Lewis (1979) A taxonomic study of the genus *Lethrinops* Regan (Pisces: Cichlidae) from Lake Malawi. Part 3. Ichthyol. Bull. *38:*1–25.

Galis, F. (1992) A model for biting in the pharyngeal jaws of a cichlid fish: *Haplochromis piceatus.* J. Theor. Biol. *155:*343–368.

Greenwood, P.H. (1959) The monotypic genera of cichlid fishes in Lake Victoria, Part II. Bull. Brit. Mus. (Nat. Hist.), Zool. *5:*163–177.

Greenwood, P.H. (1965) Environmental effects on the pharyngeal mill of a cichlid fish, *Astatoreochromis alluaudi* and their taxonomic implications. Proc. Linn. Soc. Lond. *176:*1–10.

Greenwood, P.H. (1981) The Haplochromine Fishes of the East African Lakes. München: Kraus International.

Hoogerhoud, R.J.C. (1984) A taxonomic reconsideration of the haplochromine genera *Gaurochromis* Greenwood, 1980 and *Labrochromis* Regan, 1920 (Pisces, Cichlidae). Neth. J. Zool. *34:*539–565.

Hoogerhoud, R.J.C. (1986) Taxonomic and ecological aspects of morphological plasticity in molluscivorous haplochromines (Pisces, Cichlidae), University of Leiden, Ph.D. thesis.

Huysseune, A. (1989) Morphogenetic aspects of the pharyngeal jaws and neurocranial apophysis in postembryonic *Astatotilapia elegans* (Trewavas, 1933) (Teleostei: Cichlidae). Acad. Anal., Brussels *51:*11–35.

Kollar, E.J. (1981) Tooth development and dental patterning. In T.G. Connelly, L.L. Brinkley, and B.M. Carlsson (eds): Morphogenesis and Pattern Formation. New York: Raven Press, pp. 87–102.

Kornfield, I. (1991) Genetics. In M.H.A. Keenleyside (ed.): Cichlid Fishes: Behaviour, Ecology and Evolution. London, New York: Chapman and Hall, pp. 103–128.

Kornfield, I.L., and J.N. Taylor (1983) A new species of polymorphic fish, *Cichlasoma minckleyi* from Cuatro Cienegas, Mexico (Teleostei: Cichlidae). Proc. Biol. Soc. Wash. *96:*253–269.

Kullander, S.O. (1984) Cichlid fishes from the La Plata Basin. Part V. Description of *Aequidens plagiozonatus* sp. n. (Teleostei, Cichlidae) from the Paraguay River system. Zool. Scr. *13:*155–159.

Leeson, C.R., and T.S. Leeson (1976) Histology, 3rd ed. Philadelphia: W.B. Saunders.

Lanyon, L.E., and C.T. Rubin (1985) Functional adaptation in skeletal structures. In M. Hildebrand, D.M. Bramble, K.F. Liem, and D.B. Wake (eds): Functional Vertebrate Morphology. Cambridge, MA: Belknap Press, pp. 1–25.

Lewis, D.S.C. (1982) A revision of the genus *Labidochromis* (Teleostei: Cichlidae) from Lake Malawi. Zool. J. Linn. Soc. *75:*189–265.

Liem, K.F., and P.H. Greenwood (1981) A functional approach to the phylogeny of the pharyngognath teleosts. Am. Zool. *21:*83–101.

Loiselle, P.V. (1979) A revision of the genus *Hemichromis* Peters 1858 (Teleostei: Cichlidae). Ann. M.R.A.C., In-8, Sc. Zool. *228:*1–124.

Marks, S.C., and S.N. Popoff (1988) Bone cell biology: The regulation of development, structure, and function in the skeleton. Am. J. Anat. *183:*1–44.

Martin, R.B. (1991) Determinants of the mechanical properties of bones. J. Biomech. *24:*79–88.

Meunier, F.J., and L. Trébaol (1987) Données histologiques sur les mâchoires pharyngiennes de *Trachinotus teraia* (Cuvier 1832), Carangidae (Ostéichthyen, Perciforme) d'Afrique tropicale. J. Biol. Buccale *15:*239–248.

Meyer, A. (1987) Phenotypic plasticity and heterochrony in *Cichlasoma managuense* (Pisces, Cichlidae) and their implications for speciation in cichlid fishes. Evolution *41:*1357–1369.

Meyer, A. (1989) Cost of morphological specialization: feeding performance of the two morphs in the trophically polymorphic cichlid fish, *Cichlasoma citrinellum.* Oecologia *80:*431–436.

Meyer, A. (1990a) Morphometrics and allometry in the trophically polymorphic cichlid fish, *Cichlasoma citrinellum:* Alternative adaptations and ontogenetic changes in shape. J. Zool., Lond. *221:*237–260.

Meyer, A. (1990b) Ecological and evolutionary consequences of the trophic polymorphism in *Cichlasoma citrinellum* (Pisces: Cichlidae). Biol. J. Linn. Soc. *39:* 279–299.

Nelson, G.J. (1969) Gill arches and the phylogeny of fishes, with notes on the classification of vertebrates. Bull. Am. Mus. Nat. Hist. *141:*475–552.

Sire, J.-Y. (1985) Fibres d'ancrage et couche limitante externe à la surface des écailles du Cichlidae *Hemichromis bimaculatus* (Téléostéen, Perciforme): données ultrastructurales. Ann. Sci. Nat., Zool. *7:*163–180.

Slootweg, R., P.A. Vroeg, and S.J. Wiersma (1993) Effects of molluscivorous fish, water quality and pond management on the development of schistosomiasis vector snails in aquaculture ponds. Aquacult. Fisheries Manag. *24:*123–128.

Sokal, R.R., and F.J. Rohlf (1981) Biometry. The principles and practice of statistics in biological research, 2nd ed. San Francisco: W.H. Freeman.

Trewavas, E. (1983) Tilapiine fishes of the genera *Sarotherodon, Oreochromis* and *Danakilia.* London: British Museum.

Vaes, G. (1988) Cellular biology and biochemical mechanism of bone resorption. Clin. Orthop. Rel. Res. *231:* 239–271.

Vandewalle, P., A. Huysseune, P. Aerts, and W. Verraes (1994) The pharyngeal apparatus in teleost feeding. In: Bels, V.L., M. Chardon, and P. Vandewalle (eds): Biomechanics of Feeding in Vertebrates: Advances in Comparative and Environmental Physiology, Vol. 18. Berlin: Springer-Verlag, pp. 59–92.

Wilkinson, L. (1990) SYSTAT: The System for Statistics. Evanston, IL: Systat.

Witte, F., C.D.N. Barel, and R.J.C. Hoogerhoud (1990) Phenotypic plasticity of anatomical structures and its ecomorphological significance. Neth. J. Zool. *40:*278–298.

Wonacott, T.H., and R.J. Wonacott (1977) Introductory Statistics, 3rd ed. New York: John Wiley & Sons.